An industrial streamer corona plasma system for gas cleaning

An Industrial Streamer Corona Plasma System for Gas Cleaning

G. J. J. Winands, Keping Yan, A. J. M. Pemen, *Member, IEEE*, S. A. Nair, Zhen Liu, and E. J. M. van Heesch

***Abstract*—For pulsed corona plasma applications, it becomes important to develop pilot systems with large average power and high-energy conversion efficiency. Since the beginning of 2000, we have been working on an industrial corona plasma system with tasks of 10–30 kW in average power and higher than 90% of total energy conversion efficiency. The pulsed-power source should have the following specifications: rise time of 10–25 ns, pulsewidth of 50–150 ns, pulse repetition rate of up to 1000 pulses per second, peak voltage pulse of 70 kV, peak current of 3.5 kA, dc bias voltage of 10–35 kV, and energy per pulse of up to 30 J. Sixteen parallel wire cylinder reactors are used to match the source. Gas and reactor temperatures can be controlled individually with water flow around the outside of those cylinders. The system is designed for gaseous oxidation and electrostatic dust precipitation. The system has been used for up to 17 kW in average power. This paper reports the system in detail, discusses issues related to the matching between the source and the reactor, and presents an example of industrial demonstrations on odor abatement at 1000 m^3/h. Finally, this paper also gives a general guideline for design of corona plasma systems.**

***Index Terms*—Corona, impedance matching, spark gaps, transmission lines.**

I. Introduction

AN INTERESTING technique for removal of multiple pollutants, such as volatile organic compounds (VOCs), odor, bacterias, tars, fine particles, NO_x, and SO_x, is to use streamer corona plasma [1]–[12]. Radicals produced by the discharge induce chemical reactions leading to a decrease in the pollutant concentrations. The pollutants are often converted to by-products, which are either less harmful or easy to be handled. It has been confirmed that the technique is very effective for low concentration abatement, its investment and operational costs are lower and multiple pollutants can be removed simultaneously.

The first industrial corona plasma system was reported by Ente Nazionale Energia Elettrica (ENEL) for simultaneous removal of dusts, SO_2, NO_x, and heavy metals from exhaust gases [1]. Unfortunately, lack of cost effective corona plasma generation and processing techniques discouraged industries. Nevertheless, three industrial corona plasma demonstration systems with up to 40–120 kW in average power were recently reported in Japan, Korea, and China. For example the system described by Mok *et al.* [13], with an average output power of 40 kW, or the system described by Lee *et al.* [14], with an average output power of 120 kW. All of them are based on magnetic compression techniques with pulse duration of 200–500 ns. Main drawbacks of these reported systems are their relatively low-energy conversion efficiency.

Our previous pulsed corona plasma system gives an average output power of 2 kW with a pulsewidth of 20–100 ns [15], which is too small for industrial applications. The main objective of this paper is to report a novel pulsed corona plasma system with 10–30 kW of average power, 50–100 ns of pulse duration, and 90% of energy conversion efficiency.

II. Pulsed-Power Source

For pulsed corona system, nonthermal plasma is produced by applying short high-voltage pulses onto a nonuniform electrode geometry. When the applied electric field in between the electrodes exceeds a critical value, streamers start propagating from one electrode toward the counter one. The energetic electrons ($\sim$10 eV) around the streamer head dissociate gaseous molecules, generate radicals, and then induce chemical reactions. As soon as the primary streamer bridges the gap a secondary streamer is formed, which travels only partly into the gap, and is much less energetic. As a result, fewer radicals are produced and its chemical efficiency is lower. For efficient pollutant removal, it can be stated that primary streamers are more efficient than the secondary streamers, and as soon as the primary streamers cross the electrode gap, the applied electric field should be removed. Besides this argument, several other issues also have to be considered when constructing an industrial pulsed corona system, such as output power, lifetime, reliability, safety, and energy efficiency. Generally speaking, the issue of system processing efficiency can be divided into four parts as illustrated in Fig. 1.

The first step is related to the source design. The energy from the mains has to be modulated into pulses efficiently. The second step is about the matching between the source and the reactor. The modulated pulses have to be applied efficiently to the reactor. The third one is related to plasma generation. Transferring a large amount of energy into the reactor does not necessarily imply high chemical yield. The electron energy distribution function of the generated plasma will greatly affect the processing efficiency. The homogeneity of the generated

Manuscript received August 3, 2005; revised May 31, 2006. This work was supported by the Dutch Innovatieve Onderzoeksprogramma's-Electromagnetische Vermogenstechniek (IOP-EMVT) program.

G. J. J. Winands is with the Department of Electrical Engineering, Eindhoven University of Technology, 5600 MB Eindhoven, The Netherlands (e-mail: g.j.j.winands@tue.nl).

K. Yan is with the Department of Environmental Science, Zhejiang University, Hangzhou 310027, China.

A. J. M. Pemen and Z. Liu are with the Electrical Power Systems Group, Department of Electrical Engineering, Eindhoven University of Technology, 5600 MB Eindhoven, The Netherlands.

S. A. Nair is with Tokyo Institute of Technology, Tokyo 152-8550, Japan.

E. J. M. van Heesch is with Eindhoven University of Technology, 5600 MB Eindhoven, The Netherlands.

Digital Object Identifier 10.1109/TPS.2006.881278

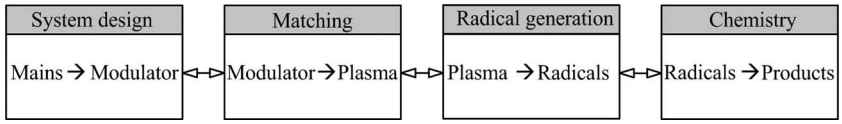

Fig. 1. Steps in optimization of energy efficiency of pulsed corona plasma system.

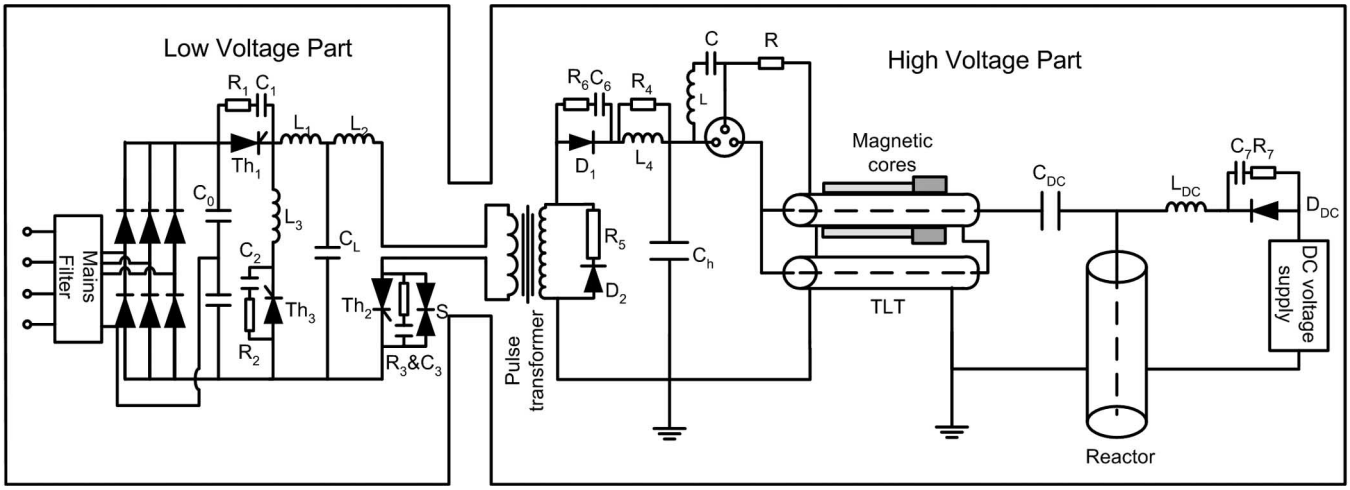

Fig. 2. Schematic overview of the HPPS, where two types of ferrites are used on the TLT to increase the secondary mode impedance and also to critically damp the oscillation after corona plasma quenching.

plasma is another important factor to influence the efficiency. The fourth step is mainly dependent on the related process. By changing process parameters, such as temperature and humidity, or by using additives and catalysts, one may optimize the induced reactions.

This paper does not intend to discuss all of the four steps in details, but to focus on the first two steps. The energy conversion efficiency of the first step is defined as the efficiency to charge the high-voltage pulse forming capacitor. It is calculated by the ratio of the energy stored inside the capacitor over the total energy input from the mains. For the present design, it is about 95% [4]. The second step is the efficiency from the modulator to the reactor, i.e., the ratio of corona energy over the stored energy. For achieving high efficiency, the output impedance of the pulse generator and the impedance of the reactor have to be properly matched. The problem here is caused by the impedance of the reactor, which is transient and nonlinear. The total energization process has to be considered, namely before, during and after streamer generation [4].

Before the applied voltage reaches the streamer inception, the reactor behaves as a capacitor with a vacuum capacitance of $C_{\rm r}$. For a power modulator generating fast rising (rise time τ) pulses, the rise time on the reactor becomes $2Z_{\rm out} \cdot C_{\rm r}$, where $Z_{\rm out}$ is the output impedance of the modulator. Simulations showed that optimal energy conversion efficiency can be achieved when the plasma is started before the moment at which the energy transfer from the source to this capacitance reaches its maximum value. The exact timing depends on the values of $C_{\rm r}$, $Z_{\rm out}$, and τ. Igniting the plasma too late will result in low-energy conversion efficiency. During streamer generation, the reactor can be depicted as a resistor $R_{\rm r}$. When $R_{\rm r} = Z_{\rm out}$, the energy efficiency reaches its maximum. It has been observed that the impedance $R_{\rm r}$ tends to decrease to the output impedance $Z_{\rm out}$ of the generator when increasing the peak voltage on the reactor. Superposition of a dc bias voltage on the voltage pulses can also be used to increase the voltage, and thus to improve the matching. After corona plasma quenching, the current rapidly drops to zero, and the reactor impedance becomes much larger than the output impedance $Z_{\rm out}$. As a result, the energy transfer stops and a high-frequency oscillation can be observed. To prevent damage of the switch as a result of this oscillation, a transmission line transformer (TLT) with two-type magnetic cores is used to absorb the reflected energy.

TABLE I
GENERAL CHARACTERISTICS OF THE HPPS SYSTEM

Average Power	10 - 30 kW	Rise time	15 ns
Max. pulse voltage	70 kV	Pulse width (power)	50 - 150 ns
Peak current	3.5 kA	Energy per pulse (EPP)	10 ~ 30 J
Pulse repetition rate	1-1000 pps	Jitter on EPP	1 ~ 2%
DC bias voltage	0-35 kV	Energy efficiency	~ 90%

A. Hybrid Pulsed-Power System (HPPS) System

Fig. 2 shows a schematic representation of the HPPS. The term hybrid was used because not only pulses are applied onto the reactor but also a dc bias voltage is used. The system is based on resonant charging of a capacitor bank $C_{\rm h}$ and subsequently discharging it via a heavy-duty spark-gap switch. The dc source not only results in an increase of the energy per pulse and an improvement of the energy efficiency, but also enables electrostatic precipitation (ESP). The general characteristics of the system are summarized in Table I.

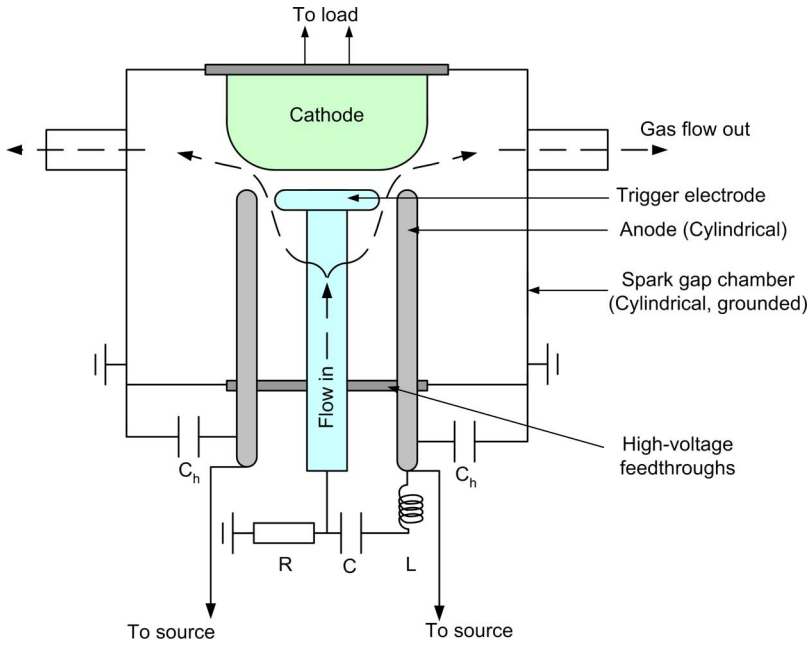

Fig. 3. Schematic drawing of the spark gap switch, including the LCR trigger circuit. The high-voltage capacitors $C_{\rm h}$ are positioned coaxially around the spark gap to reduce the inductance. The distance between the anode and the trigger electrode is $\sim$0.3 mm. The surface of the cathode is $\sim$12 cm^2; the cathode–anode distance is 3 mm. The design of the switch is completely coaxial. There are six outlets for flush gas flow, positioned in a starlike configuration. (Color version available online at http://ieeexplore.ieee.org.)

1) Voltage Pulse Generator: With regard to the circuit in Fig. 2: the coupling capacitor $C_{\rm DC}$ separates the circuit into two parts. The left side is the voltage pulse modulator, and the right side is the dc source. The low-voltage part consists of a mains filter, a set of rectifiers, three air-core inductors (10–30 μH), three thyristors, and two energy storage capacitors ($C_0 = 2{-}3$ mF). The three thyristors are switched consecutively in order to resonantly charge $C_{\rm h}$. The third thyristor is used to stabilize the voltage on $C_{\rm L}$, which results in an output with a jitter of less than 1% [4]. The pulsewidth, the output voltage and current pulses of the low-voltage part are around 25 μs, 1 kV, and 1 kA, respectively. A step-up pulse transformer is used to increase the voltage pulse to 36 kV. For proper matching between the low- and the high-voltage parts, the values of $C_{\rm L}$ and $C_{\rm h}$ obey the equation of $C_{\rm L} = N^2 C_{\rm h}$, where $N = 36$ is the transformer ratio.

The most critical component of the voltage pulse generator is the heavy-duty switch used to discharge the high-voltage capacitor $C_{\rm h}$ into the TLT. The switch should satisfy the following requirements: high hold-off voltage, nanosecond switching time, an impedance that matches the input of the TLT, high switching current, high pulse repetition rate, low losses, long lifetime, cost effective, compact, and insensitive to occasional over voltage/current. In our opinion, advanced spark-gap switches do match those specifications. For the present HPPS system, a high-pressure spark-gap switch with switching voltage of 40 kV, switching current of 4 kA, and pulse repetition rate of 1000 pps is used. Its main specifications are illustrated in Fig. 3. The switch can be pressurized up to 4 bars, and is flushed with dry air of up to 35 N $\cdot$ m^3/h to improve the recovery time [16]. Copper-tungsten alloy is used as electrode material. The estimated lifetime is in the range of $10^9{-}10^{10}$ shots at 10 J/pulse. It was constructed coaxially to make its impedance equal to the input impedance of the TLT. Such optimal design creates short arcs, which dissipate less energy and have lower inductance [17].

For stable operation, the switch should close just after the high-voltage capacitor is charged. Prefiring decreases the average switching voltage, and thus causes a decrease of the energy. Late firing implies long-period stress on the high-voltage components, and limits the pulse repetition rate. With regard to the circuit in Fig. 2, the triggering is performed with an LCR trigger method, where a 10-μH inductor, a 450-pF capacitor, and a 1.2-MΩ resistor form the trigger circuit. Details were reported earlier [4], [18].

After the switch closes, the capacitor $C_{\rm h}$ is discharged into a two stage TLT, which has an input and output impedance of $Z_0/2$ and $2Z_0$, respectively. The TLT was constructed from concentric metal tubes with $Z_0 \sim 10\ \Omega$, and it is filled with transformer oil. For large average output power and short pulsewidths, it is preferable to keep the output impedance of the source ($Z_{\rm out}$) as low as possible. For a capacitor discharge, the pulsewidth is roughly equal to $Z_{\rm out} \cdot C_{\rm h}$. For high average power, $C_{\rm h}$ has to be large, thus $Z_{\rm out}$ should be small. A TLT usually consists of a set of transmission lines connected in series or in parallel configurations at its ends. It can be used for several purposes, such as to match impedances and to multiply voltage and/or current. Very detailed discussions can be found in [19]. For the present system, it is used to increase the output voltage. The ideal gain of an n-stage TLT is equal to its line number n. In practice, the gain is a little smaller. To minimize the losses, the secondary mode impedance $Z_{\rm s}$, which is defined as the characteristic impedance between the outer conductor of the upper cable and the ground structure, has to be as large as possible. The corresponding current is called secondary mode current. The secondary mode current has to be as small as

possible in order to achieve an optimal gain and high-energy efficiency. In practice, this is often accomplished by placing magnetic cores around the upper stages of the TLT.

2) DC Bias Power Source: A 1–2-mH ferrite core inductor $L_{\rm dc}$ is used to decouple the voltage pulse from the dc. In order to avoid spark breakdown, the dc base voltage is limited to 30 kV for the present system. When using the dc source, two sources will energize the reactor independently. Before a high-voltage pulse is applied, the reactor is charged to $V_{\rm dc}$ by the dc source in about 100 μs via a charging diode $D_{\rm dc}$, inductor $L_{\rm dc}$, coupling capacitor $C_{\rm dc}$ (14 nF), and the TLT. When the spark gap is fired, the energy stored in both $C_{\rm dc}$ and $C_{\rm h}$ is transferred to the reactor simultaneously. After plasma generation, the reactor is charged again by the dc source. During the pulsed energization, streamer corona plasma is generated; and in between pulses ESP can be realized.

B. Streamer Corona Plasma Reactor

For industrial applications, wire-cylinder, wire-plate, or multipoint-plate configurations are commonly used. The electrode gap distance and electrode(s) curvatures are determined by the output voltage of the source. Ideally, the streamers should cross the electrode gap completely. This requires a minimum voltage and pulsewidth. For industrial applications, the electrode gap distance is preferred to be large. The distance, however, is limited because pulsed-power sources with extreme high-voltage output are expensive. The length of the high-voltage electrode depends on the required energy and on the type of processes. For nontermination processes [4] radicals mainly react with pollutants. In this case, the removal efficiency linearly increases with applied energy, and the process does not depend on the residence time. A smaller reactor with higher energy density per pulse per unit length of the reactor can be adopted. For nonlinear termination processes, however, radicals mainly terminate due to reactions between themselves. In this case, it is preferable to increase the reactor volume and to reduce the energy density per pulse and per unit volume of the reactor. This is also true for particle collection. Specific guidelines for designing the reactor can be found in [24].

The reactor of the HPPS consists of 16, vertically positioned, wire-cylinder reactors in parallel. The wire diameter is 3 mm. The length and diameter of each reactor are 1000 and 160 mm, respectively. This results in a total reactor volume of 0.32 m^3. The reactor is constructed from stainless steel to prevent degeneration as a result of chemical attack from the created acids. The outside of the cylinders can be cooled with water. Gaseous inlet and outlet are located at the bottom and the upper of the reactor, respectively. The reactor is energized from its top with a maximum energy per pulse per meter of 2 J.

III. Results and Discussions

To evaluate the voltage and the current waveforms at the input of the reactor, the experimental set-up is equipped with differentiating–integrating (D–I) measuring systems [20]. A digital oscilloscope (1 GHz, 4 GS/s) is used to record the measured signals. The power waveform is determined as the product of the voltage and current waveforms. The energy is calculated by integrating the power waveform. Fig. 4 shows the results.

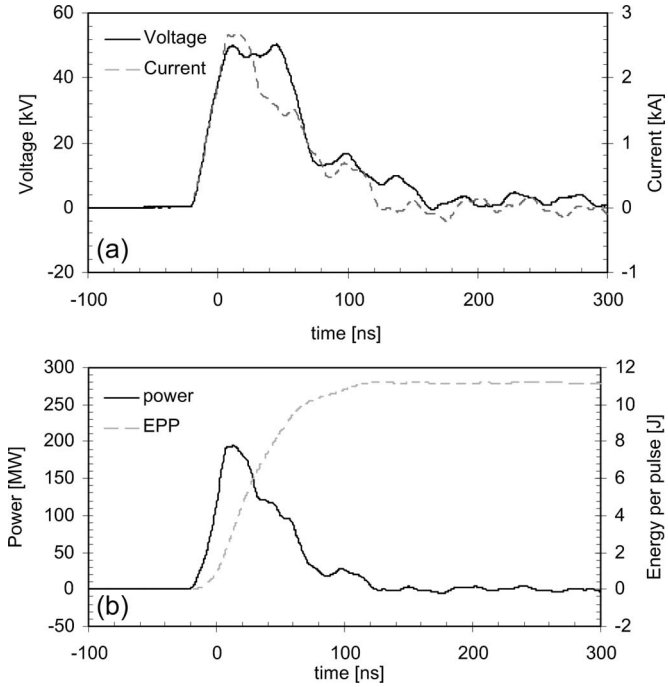

Fig. 4. Typical electrical waveforms on the reactor. The graphs are the result of averaging over 1000 pulses. During the measurements: $C_{\rm L} \sim 13$ μF and $C_{\rm h} \sim 10.6$ nF, pulse repetition rate of 1000 pps.

The rise time of the pulse on the reactor, the time required for the voltage to rise from 10% to 90% of its maximal value, is about 16 ns (equivalent 1/e-time is 12 ns). As expected, the rise time does not depend on the energy per pulse, dc bias voltage and pulse repetition rate since the rise time (1/e-time) of the voltage on the reactor is equal to $2Z_{\rm out}C_{\rm r}$ (assuming that the pulses generated by the source have rise-times $\ll 2Z_{\rm out}C_{\rm r}$). The reactor capacitance $C_{\rm r}$ was determined to be 320 pF. Combined with the output impedance $Z_{\rm out}$ of 20 Ω this gives a rise time of 13 ns which is close to the experimental value. The agreement between experiment and theory indicates that the rise time of the pulses generated by the power modulator is much smaller than the characteristic rise time of the voltage on the reactor load. The pulsewidth [full-width at half-maximum (FWHM)] is around 50–60 ns. It was observed that the pulsewidth depends on the energy per pulse, as can be expected for a capacitor discharge.

In Fig. 5(a), it can be seen that the peak power on the reactor increases as a function of the dc bias $V_{\rm dc}$. Because the energy per pulse is the time integral of the power waveform, it is obvious that the energy per pulse also increases. This increase is due to the following two factors. First, as expressed by (1), there is more stored energy $E_{\rm dc}$ in the coupling capacitor $C_{\rm dc}$ and in the reactor:

$$E_{\rm dc} = \frac{1}{2}(C_{\rm dc} + C_r)V_{\rm dc}^2. \tag{1}$$

Second, by increasing the dc bias voltage, more of the stored energy in $C_{\rm h}$ can be transferred to the reactor as a result of improved matching. This phenomenon can be observed by

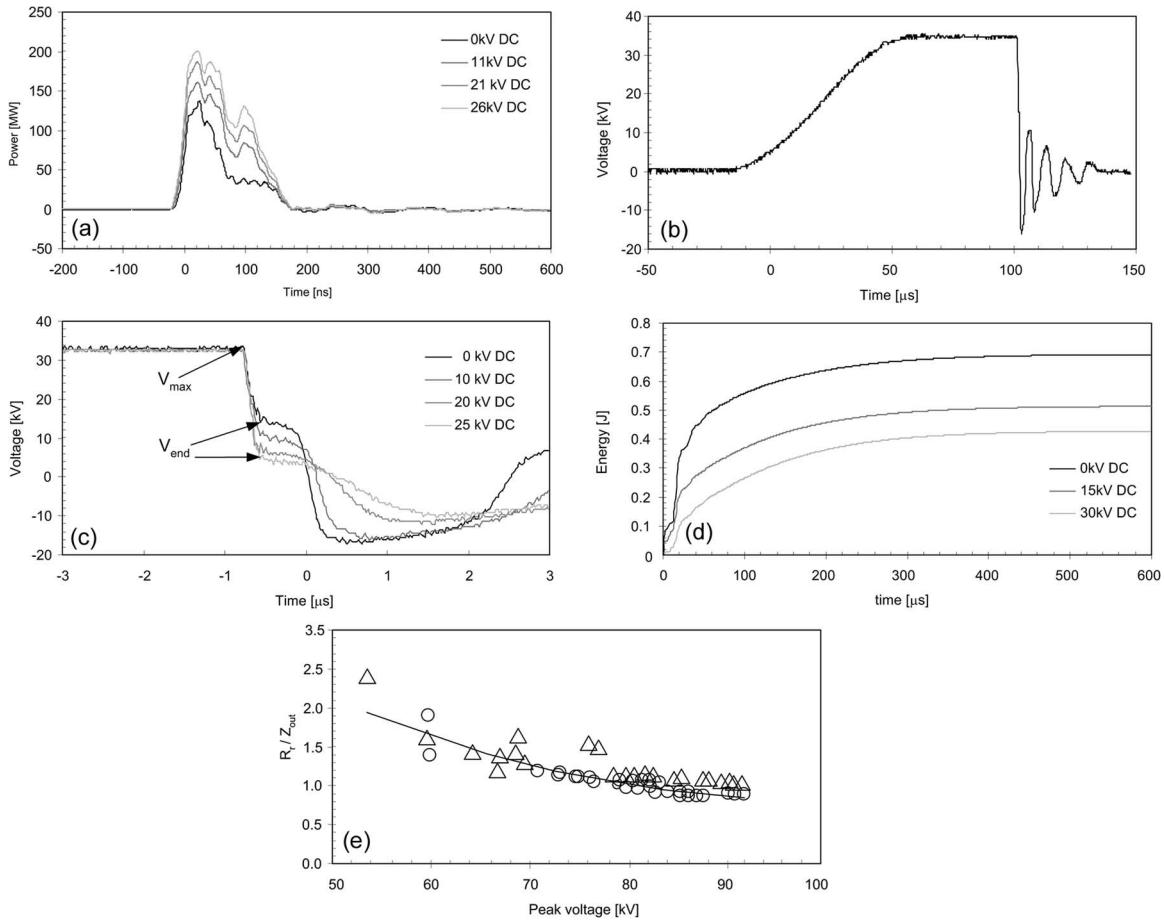

Fig. 5. (a) Power waveforms as function of the dc bias voltage, $C_{\rm h} = 10.6$ nF. (b) Voltage waveform on $C_{\rm h}$ ($= 25.8$ nF), single-shot measurement without dc bias voltage. (c) Voltage waveforms on $C_{\rm h}$ after the spark-gap fires as function of dc bias voltage level, single-shot measurements. (d) Energy dissipation in R_5 resistor as function of the dc bias voltage, $C_{\rm h} = 10.6$ nF. (e) The ratio of the reactor impedance over the output impedance as function of applied voltage. The reactor impedance is defined as the ratio of voltage over current at the moment the current reaches its maximum value. Two reactor configurations were used, both wire-cylinder type. Length, wire diameter and cylinder diameter are 3000, 3, and 160 mm for the circles, and 3000, 1, and 250 mm for the triangles, respectively. The solid line is an interpolation of the measuring results.

studying the voltage waveforms on $C_{\rm h}$ as shown in Fig. 5(b) and (c). The capacitor is resonantly charged in about 50 μs to its maximum $V_{\max}$. The voltage, then, remains almost constant until the spark-gap switch is fired. Some ringing occurs after the switch is closed due to the mismatch. Fig. 5(c) replots the waveforms on a short time scale. One can easily see that the capacitor does not discharge completely, but to a residual voltage $V_{\rm end}$, indicating that not all of the stored energy can be transferred into the reactor within the short duration. Thus, the energy from $C_{\rm h}$ used for the plasma generation becomes

$$E_{C_{\rm h}} = \frac{1}{2} C_{\rm h} \left(V_{\max}^2 - V_{\rm end}^2 \right). \tag{2}$$

By superimposing a dc bias voltage, both the residual voltage $V_{\rm end}$ and its ringing decrease, and thus much more energy is transferred to the reactor. Obviously, the matching is improved. Besides the economical advantage of having more energy going from $C_{\rm h}$ into the reactor, there is also the advantage of decreased component wear. Most of the energy that does not go into the reactor is dissipated in the spark-gap switch, the TLT and in the $D_2 - R_5$ circuit. An example of the energy dissipation in R_5 is shown in Fig. 5(d). We also observed that either increasing the dc bias voltage or pulse voltage amplitude can lead to an improvement in matching. A typical example is shown in Fig. 5(e) [4]. Clearly, for sufficiently high voltage, the reactor impedance becomes equal to the output impedance of the source and the energy transfer can thus be optimized. It seems that the plasma generation is automatically adjusted to match the available energy stored in the capacitors. Changes in plasma generation as a function of the applied voltage have already been observed [21] using a fast intensified charge-coupled device (CCD) camera. It is believed that changes in streamer diameter, velocity, and branching lead to the automatic impedance matching.

The results shown in Fig. 6 summarize the experiments performed to optimize the output power and the energy efficiency. The experiments were carried out during 5-min test cycles. Long duration experiments were also performed. It was observed that the jitter in average output energy was about 1%–2%. No problems occurred during the long duration operation. The output power is varied by varying the pulse repetition rate, the $C_{\rm h}$ value, and the dc-bias voltage. The results are summarized in Fig. 6(a) with a maximum average power of 17 kW. The energy per pulse decreases slightly as function of pulse repetition rate due to the small value of the primary energy storage capacitor C_0.

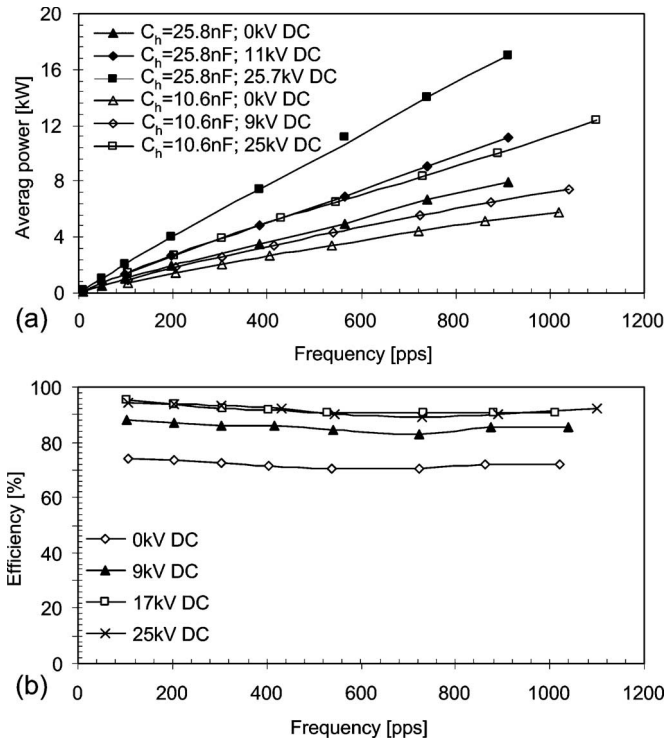

Fig. 6. Average power and energy conversion efficiency via the pulse repetition rate, where standard-deviation evaluation is less than 1% and $C_{\rm h} = 10.6$ nF.

The energy efficiency (of the second step in the chain depicted in Fig. 1) is defined as the ratio of primary stored energy over the corona energy as

$$\eta = \frac{\int V_{\rm reactor} \cdot I_{\rm reactor} dt}{\frac{1}{2}(C_{\rm DC} + C_{\rm r})V_{\rm dc}^2 + \frac{1}{2}C_{\rm h}V_{\rm max}^2}. \tag{3}$$

It does not depend on the pulse repetition rate, but increases with dc bias voltage due to the improved matching. A maximum energy efficiency of about 95% was obtained. Considering a 95% of the efficiency from the mains to the $C_{\rm h}$, we can conclude that the total energy conversion efficiency is about 90%. For the 120 kW average power modulator described in [14], the efficiency is about 50%. The 40-kW average power modulator described in [13] has a efficiency of less then 76%; and for the system described in [22], it is less then 50% for 1–2 kW average power. All systems have considerably lower energy transfer efficiency than the presented one. Part of the difference between the efficiency of these systems is due to the use of magnetic pulse compression technique. The other difference is due to the system design and matching.

TABLE II
GCMS MEASUREMENTS FOR VOC ABADEMENT

Group	Chemical compound	Input concentration [μg/m^3]	Output concentration [μg/m^3]
Aromatic CHs	Benzene	18	7
	Toluene	358	1
	Ethylbenzene	8	0
	Styreen	11	0
	Ethynylbenzene	0	2
Cyclic CHs	Methylcyclopentane	51	0
	Cyclohexane	15	0
Aliphatic CHs	Heptane	12	1
	Octane	3	1
	Nonane	4	9
	Decane	4	0
	Undecane	4	0
	Dodecane	3	0
	Hexane	114	0
	2-methylpentane	125	0
	1-nonane	0	1
Alchohol	Ethanol	693	0
	1-butanol	1	0
	2-methyl-1-butanol	69	0
	3-methyl-1-butanol	24	0
	phenol	0	24
Esters	Benzoate	0	263
Ketones	Acetone	2481	90
	2-butanon	1329	28
	3-methyl-2-butanon	2	0
	2-octanon	3	0
	acetofenon	65	108
	5-nonanon	1	0
	3-fenyl-2,5-furanedion	0	42
	2-methylcyclopentanon	0	1
	1,3-isobenzofuranedion	0	3
Aldehydes	Acetaldehyde	705	76
	Benzaldehyde	85	223
	3-methylbutanal	46	0
	2-methylbutanal	54	0
	Hexanal	50	6
	Heptanal	7	5
	Octanal	0	168
	Decanal	0	21
	Fenylavetaldehyde	0	35
	Endecanal	0	4
Cl	Dichloromethane	175	0
components	Tetrachlorocarbon	8	0
	Chloroform	17	0
Organic	Dimethylsulfide	741	0
sulphur	Carbondisulfide	248	2
	Dimethyldisulfide	1324	0
	Methylthiophene	44	0
	Thiophene	6	0
Furans	3-methylfuran	66	0
	Furane	0	10
Terpens	Alpha-pinene	9	0
	Limonene	4	0

A. Industrial Demonstration on Odor Emission Abatement

As an example of industrial applications of the HPPS system, Table II lists results of an industrial demonstration on odor emission abatement for a Dutch compost manufacturer. The experiments were performed as a feasibility study to evaluate simultaneous removal of various gaseous compounds and the present system design. Fig. 7 shows a diagram of the related production process. An acid washer and a biobed filter were already used, but their performance did not match the emission regulation. The total flow rate of the exhaust gas is about 250 000 N $\cdot$ m^3/h. Though our plasma system could be installed at three locations as indicated in Fig. 7, we mainly focused on its performance where odor concentrations are high, i.e., position one, just after the manufacturing process. The demonstration was performed with a substream gas flow of

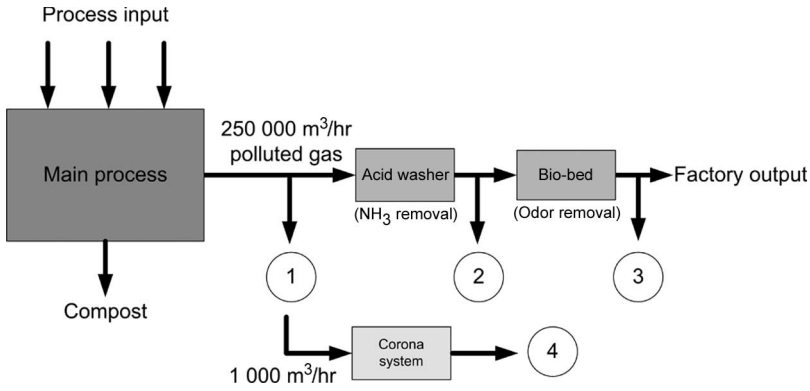

Fig. 7. Process overview of compost manufacturer.

1000 $N \cdot m^3/h$, and with a corona energy per pulse of 8 J, a pulse repetition rate of 250 pps, a peak-voltage on the reactor of 70 kV, a peak current of 3 kA, a pulsewidth (FWHM) of 75 ns, and a rise time of the voltage pulse of 16 ns. The total corona plasma power is 2 kW, resulting in a corona energy density of 7.2 J/L. The residence time of the gas inside the reactor was 1.2 s. The gas temperature was about 30 °C–40 °C, the relative humidity was higher than 80%. The demonstration lasted several hours continuously without any problem.

Chemical analyses were performed by a certified lab, PRA OdourNet BV. For the analyses, 40 L of gases from the output of the reactor were sampled in nalophene bags in 30-min experimental measuring cycles. The bag was placed inside a low-pressure container. The gas is sampled according to the "lung-method" to prevent the odorous gases to come into direct contact with the pump. To prevent condensation inside the bags and its related absorption, the sampled gas was diluted with nitrogen. Several techniques were used for gaseous analysis. The Impinger method was used to determine H_2S concentration. A gas chromatograph mass spectrometer (GCMS) was used to determine VOCs concentrations. The GCMS consists of a Varian 2700 gas chromatograph and a MAT 112S Finnigan mass spectrometer.

The removal efficiency of H_2S exceeded 95% (initial concentration 15.3 $\mu g/m^3$, output concentration below detection limit of 0.8 $\mu g/m^3$). Table II presents the results for VOC removal in terms of initial and final concentrations. One can easily see that multiple gases can be removed simultaneously. Aldehydes are the most difficult ones to be removed. Esters on the other hand, are produced by the plasma treatment. We also observed that the plasma leads to a certain amount of ozone slip when increasing the plasma power.

In comparison with Wang's [23] work (H_2S removal under a gas flow rate of 5.7 m^3/min, less than 76.0 $\mu g/m^3$ of H_2S, a discharge power of 1.2 kVA, a removal efficiency of 95%, and a corona energy of 12.6 J/L), the present system has an energy consumption of about 57% of the reported one. Although pollutant removal efficiency is usually dependent on initial pollutant concentration, and as a consequence the obtained H_2S removal efficiency cannot be compared directly to the work of Wang, in general removal efficiency decreases for decreasing concentrations. The obtained decrease of energy consumption is thus a lower threshold value.

IV. Conclusion

DC bias superimposed pulse energization leads not only to an increase of the energy per pulse but also to an improvement of the matching between reactor and power source. Industrial plasma systems with 90% energy conversion efficiency can be designed by following the proposed guidelines. Industrial demonstration on odor emission abatement for a Dutch compost manufacturer proved the design and also confirmed the feasibility of simultaneous removal of multiple compounds.

Acknowledgment

The authors would like to thank H. Bonne, F. van Gompel, H. van Leuken, and A. van Iersel for their support.

References

[1] G. Dinelli, L. Civitano, and M. Rea, "Industrial experiments on pulse corona simultaneous removal of NO_x and SO_2 from flue gas," *IEEE Trans. Ind. Appl.*, vol. 26, no. 3, pp. 535–541, May/Jun. 1990.

[2] B. Eliasson and U. Kogelschatz, "Nonequilibrium volume plasma chemical processing," *IEEE Trans. Plasma Sci.*, vol. 19, no. 6, pp. 1063–1077, Dec. 1991.

[3] R. Hackam and H. Akiyama, "Air pollution control by electrical discharges," *Eur. Phys. J. Appl. Phys.*, vol. 7, no. 1070–9878, pp. 654–683, 2000.

[4] K. Yan, E. J. M. van Heesch, and A. J. M. Pemen, "Corona induced non-thermal plasma for pollution control and sustainable technology," presented at the 8th Int. Conf. Electrostatic Precipitation, Birmingham, AL, 2001, Paper C3-1.

[5] G. J. J. Winands, K. Yan, S. A. Nair, A. J. M. Pemen, and E. J. M. van Heesch, "Evaluation of corona plasma techniques for industrial applications: HPPS and DC/AC systems," *Plasma Processes Polymers*, vol. 2, no. 3, pp. 232–237, 2005.

[6] T. Yamamoto and S. Futamura, "Nonthermal plasma processing for controlling volatile organic compounds," *Combust. Sci. Technol.*, vol. 133, no. 1–3, pp. 117–133, 1998.

[7] S. A. Nair, K. Yan, A. J. M. Pemen, G. J. J. Winands, F. M. van Gompel, H. E. M. van Leuken, E. J. M. van Heesch, K. J. Ptasinski, and A. A. H. Drinkenburg, "A high-temperature pulsed corona plasma system for fuel gas cleaning," *J. Electrost.*, vol. 61, no. 2, pp. 117–127, Jun. 2004.

[8] J. S. Clements, A. Mizuno, W. C. Finney, and R. H. Davis, "Combined removal of SO_2, NO_x, and fly ash from simulated flue gas using pulsed streamer corona," *IEEE Trans. Ind. Appl.*, vol. 25, no. 1, pp. 62–69, Jan./Feb. 1989.

[9] H. H. Kim, "Nonthermal plasma processing for air-pollution control: A historical review, current issues, and future prospects," *Plasma Processes and Polymers*, vol. 1, no. 2, pp. 91–110, Feb. 2004.

[10] S. Masuda, S. Hosokawa, X. Tu, and Z. Wang, "Novel plasma chemical technologies—PPCP and SPCP for control of gaseous pollutants and air toxics," *J. Electrost.*, vol. 34, no. 4, pp. 415–438, May 1995.

[11] H. S. B. Elayyan, A. Bouziane, and R. T. Waters, "Theoretical and experimental investigation of a pulsed ESP," *J. Electrost.*, vol. 56, no. 2, pp. 219–234, Sep. 2002.
[12] N. Klippel, "The influence of high-voltage pulse parameters on corona current in electrostatic precipitators," *J. Electrost.*, vol. 49, no. 1/2, pp. 31–49, May 2000.
[13] Y. S. Mok, H. W. Lee, and Y. J. Hyun, "Flue gas treatment using pulsed corona discharge generated by magnetic pulse compression modulator," *J. Electrost.*, vol. 53, no. 3, pp. 195–208, Sep. 2001.
[14] Y. H. Lee, W. S. Jung, Y. R. Choi, J. S. Oh, S. D. Jang, Y. G. Son, M. H. Cho, W. Namkung, D. J. Koh, Y. S. Mok, and J. W. Chung, "Application of pulsed corona induced plasma chemical process to an industrial incinerator," *Environ. Sci. Technol.*, vol. 37, no. 1, pp. 2563–2567, Jun. 2003.
[15] K. Yan, E. J. M. van Heesch, A. J. M. Pemen, P. A. H. J. Huijbrechts, F. M. van Gompel, Z. Matyas, and H. van Leuken, "A 2.0 kW pulsed corona system for inducing chemical reactions," in *Proc. IEEE Ind. Appl. Conf.*, Rome, Italy, Oct. 2000, pp. 592–599.
[16] W. J. Thayer, V. C. H. Lo, and A. K. Cousins, "Recovery of a high pulse rate spark gap switch," in *Proc. 18th IEEE Power Modulator Symp.*, 1988, pp. 257–264.
[17] P. Persephonis, K. Vlachos, C. Georgiades, and J. Parthenios, "The inductance of the discharge in a spark gap," *J. Appl. Phys.*, vol. 71, no. 10, pp. 4755–4762, May 1992.
[18] G. J. J. Winands, Z. Liu, A. J. M. Pemen, E. J. M. van Heesch, and K. Yan, "Long life-time, triggered, spark-gap switch for repetitive pulse power applications," *Rev. Sci. Instrum.*, vol. 76, no. 8, p. 085107, Aug. 2005.
[19] P. W. Smith, *Transient Electronics, Pulsed Circuit Technology*. U.K.: Wiley, 2002.
[20] A. P. J. van Deursen, H. W. M. Smulders, and R. A. A. de Graaff, "Differentiating/integrating measurement setup applied to railway environment," *IEEE Trans. Instrum. Meas.*, vol. 55, no. 1, pp. 316–326.
[21] T. M. P. Briels, E. M. van Veldhuizen, and U. Ebert, "Branching of positive discharge streamers in air at varying pressures," *IEEE Trans. Plasma Sci.*, vol. 33, no. 2, pp. 264–265, Apr. 2005.
[22] A. Pokryvailo, Y. Yankelevich, M. Wolf, E. Abramzon, S. Wald, and A. Welleman, "A high-power pulsed corona source for pollution applications," *IEEE Trans. Plasma Sci.*, vol. 32, no. 5, pp. 2045–2054, Oct. 2004.
[23] Y. Wang, "Odor gas reduction using silent and corona discharge plasma—An experimental study of non-thermal plasma techniques in pollution control," Ph.D. dissertation, Univ. Minnesota, Minneapolis, MN, 2001.
[24] K. Yan, "Corona plasma generation," Ph.D. dissertation, Eindhoven Univ. Technol., Eindhoven, The Netherlands, 2001.

G. J. J. Winands was born in Kerkrade, The Netherlands, in 1978. He received the M.Sc. degree in applied physics from the Eindhoven University of Technology, The Netherlands, in 2002.

In 2002, he joined the faculty of Electrical Engineering at the Eindhoven University of Technology. His Ph.D. work focuses on the interaction between power modulator and plasma generation/chemical processing. His interests are related to repetitive plasma generation for industrial scale gas-cleaning applications.

Keping Yan received the B.S. and M.S. degrees in applied physics from Beijing Institute of Technology, Beijing, China, and the Ph.D. degree, which focused on corona plasma generation, from Eindhoven University of Technology, Eindhoven, The Netherlands, in 1983, 1986, and 2001, respectively.

In 2006, he joined the Department of Environmental Science, Zhejiang University, Hangzhou, China, as a Full Professor. In 2004, he became a Board Member of the International Society for Electrostatic Precipitation. He is the coauthor of approximately 40 papers in journals and the holder of ten patents. Since 1988, his research interests have included applied plasma technology, corona applications, and pulsed-power sources.

A. J. M. Pemen (M'98) received the B.Sc. degree from the College of Advanced Technology, Breda, The Netherlands, in 1986 and the Ph.D. degree in electrical engineering from the Eindhoven University of Technology, The Netherlands, in 2000, both in electrical engineering.

Before joining the Electrical Power Systems Group (EPS), Eindhoven University of Technology in 1998 as an Assistant Professor, he was with KEMA T&D Power, Arnhem, The Netherlands. He is currently involved in research on pulsed-power and pulsed plasma. His research interest includes high-voltage engineering, pulsed-power, plasmas, and renewable energy systems. Among his achievements are the development of an on-line monitoring system for partial discharges in turbine generators, a pulsed-corona system for industrial applications, and a pulsed corona tar cracker. He is the Founder of the Dutch Generator Expertise-Center.

S. A. Nair was born in India, in 1978. He received the B.S. in chemical engineering from the Institute of Chemical Technology, University of Mumbai, Mumbai, India, and the Ph.D. degree from the Eindhoven University of Technology, Eindhoven, The Netherlands, in 2000 and 2004, respectively.

Since 2004, he has been a Japan Society for Promotion of Science Research Fellow with the Tokyo Institute of Technology, Tokyo, Japan. His research interests include understanding the chemical processes in nonthermal plasma-assisted catalytic fuel reforming (methane and biofuels) and nonthermal plasma-assisted gas cleaning, with focus on developing catalysts, kinetic modeling, and design of reactors.

Zhen Liu was born in Xiangcheng, China, in 1978. He received the B.S. degree from the Department of Electronic Science and Technology, Xi'an Jiaotong University, China, in 2000 and the M.S. degree from the Electrical Department, Tsinghua University, China, in 2003. He is currently working toward the Ph.D. degree at the Electrical Power Systems Group (EPS), Technische Universiteit Eindhoven (TU/e), The Netherlands.

His research interest is repetitive multiple-switch pulsed-power generation.

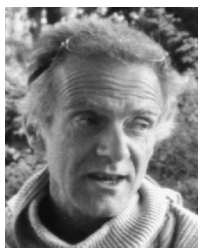

E. J. M. van Heesch was born in Utrecht, The Netherlands, in 1951. He received the Master's degree in physics from the Eindhoven University of Technology, The Netherlands, and the Ph.D. degree in plasma physics and fusion related research from the University of Utrecht, The Netherlands, in 1975 and 1982, respectively.

Since 1986, he has been an Assistant Professor at the Eindhoven University of Technology. Here, he is leading pulsed-power research. He was previously involved with shock-tube gas dynamics (Eindhoven, 1975) and with fusion technology (Jutphaas, The Netherlands, 1975–1984, Suchumi former USSR, 1978 and Saskatoon, Canada, 1984–1986). Among his designs are various plasma diagnostics, a toroidal fusion experiment, substation high-voltage measuring systems and systems for pulsed-power processing. He organizes many projects with industry and national and European Union research agencies. His research is the basis for teaching and coaching university students and Ph.D. candidates. He is a Coinventor of several patents and has coauthored more than 100 publications.